

UNCLASSIFIED

---

AD 296 133

*Reproduced  
by the*

ARMED SERVICES TECHNICAL INFORMATION AGENCY  
ARLINGTON HALL STATION  
ARLINGTON 12, VIRGINIA



---

UNCLASSIFIED

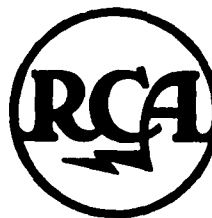
NOTICE: When government or other drawings, specifications or other data are used for any purpose other than in connection with a definitely related government procurement operation, the U. S. Government thereby incurs no responsibility, nor any obligation whatsoever; and the fact that the Government may have formulated, furnished, or in any way supplied the said drawings, specifications, or other data is not to be regarded by implication or otherwise as in any manner licensing the holder or any other person or corporation, or conveying any rights or permission to manufacture, use or sell any patented invention that may in any way be related thereto.

63-2-4

AFCH 2-918

CATALOGED BY ASTIA  
AS AD 1929613

296 133



# RADIO CORPORATION OF AMERICA RCA LABORATORIES

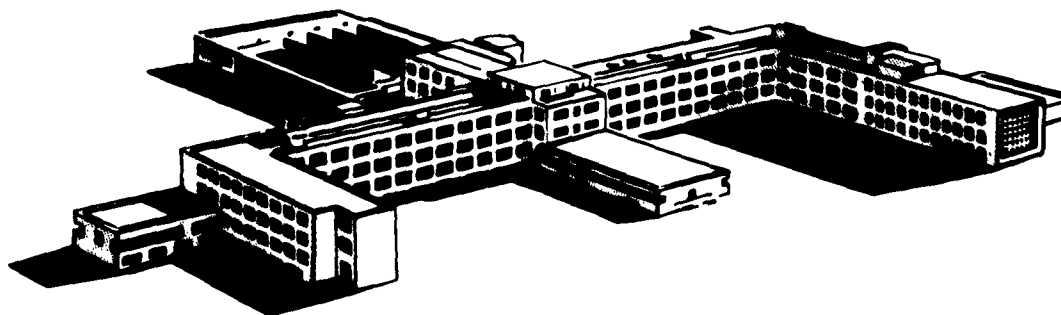
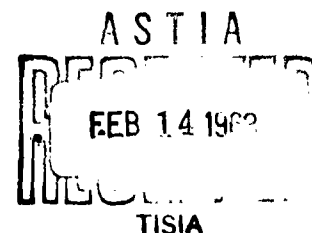
SCIENTIFIC REPORT NO. 2

## THEORETICAL AND EXPERIMENTAL STUDY OF THE COMBINED HALL-MAGNETO RESISTANCE EFFECT

CONTRACT NO. AF19(628)262

PREPARED FOR  
ELECTRONICS RESEARCH DIRECTORATE  
AIR FORCE CAMBRIDGE RESEARCH LABORATORIES  
OFFICE OF AEROSPACE RESEARCH  
UNITED STATES AIR FORCE  
BEDFORD, MASSACHUSETTS

REPORT DATE: OCTOBER 31, 1962



DAVID SARNOFF RESEARCH CENTER  
PRINCETON, NEW JERSEY

Requests for additional copies by Agencies of the Department of Defense, their contractors, and other Government agencies should be directed to the:

**ARMED SERVICES TECHNICAL INFORMATION AGENCY  
ARLINGTON HALL STATION  
ARLINGTON 12, VIRGINIA**

Department of Defense contractors must be established for ASTIA services or have their "need-to-know" certified by the cognizant military agency of their project or contract.

SCIENTIFIC REPORT NO. 2

*For the Period*

November 1, 1961 to October 31, 1962

*Report Date:* October 31, 1962

**THEORETICAL AND EXPERIMENTAL STUDY  
OF THE COMBINED HALL-MAGNETO  
RESISTANCE EFFECT**

**CONTRACT NO. AF19(629)262**

*Prepared for*

**ELECTRONICS RESEARCH DIRECTORATE  
AIR FORCE CAMBRIDGE RESEARCH LABORATORIES  
OFFICE OF AEROSPACE RESEARCH  
UNITED STATES AIR FORCE  
BEDFORD, MASSACHUSETTS**

*Work Done by:* K.K.N. Chang  
P.E. Chase  
N.J. Kolettis  
H.J. Prager  
C.F. Stocker

*Report Prepared by:* K.K.N. Chang  
P.E. Chase  
H.J. Prager

*Prepared by*

**RADIO CORPORATION OF AMERICA  
RCA LABORATORIES  
PRINCETON, NEW JERSEY**

## **ABSTRACT \***

A new group of microwave devices based on the Hall-Effect is being sought. Following a preliminary study of a 2 mc amplifier, with an electronic gain of 43 db, a frequency converter at the S-Band region of the microwave spectrum was built and gave a conversion loss of 20 to 30 db. Attempts are being made to combine the Hall sample with special materials such as rutile or YIG to achieve better conversion gain by improving the coupling to the r.f. magnetic fields. A novel scheme based entirely on enhanced interaction between the Hall sample and its associated circuitry was proposed and analytically examined. The first experimental embodiment of this proposed scheme seems to have yielded a small net gain at a frequency of 3730 mc. The report also includes the results of various experiments on microwave Hall-Effect isolators, as well as on fabrication techniques for millimeter wave tunnel diodes. These tunnel diodes have been operated as detectors at a frequency of 55 Gc. An improvement in sensitivity of 25 db as compared to ordinary crystal detectors has been obtained.

---

\* Catalog cards with an unclassified abstract may be found in the back of this document.

## TABLE OF CONTENTS

	<i>Page</i>
<b>ABSTRACT</b> .....	<i>iii</i>
<b>I. SUMMARY</b> .....	1
<b>II. HALL-EFFECT DEVICES</b> .....	3
A. LOW-FREQUENCY SCHEME .....	3
B. MICROWAVE CONVERTERS .....	8
C. ENHANCED HALL-EFFECT AMPLIFIER .....	18
D. ISOLATOR .....	24
<b>III. TUNNEL DIODES FOR MILLIMETER WAVE FREQUENCIES</b> .....	27
A. FABRICATION AND TECHNOLOGY OF TUNNEL DIODES .....	27
B. MILLIMETER WAVE TUNNEL-DIODE DETECTOR .....	29

## **I. SUMMARY**

This technical report covers work done under Contract No. AF19(628)-262 entitled "Theoretical and Experimental Study of Combined Hall-Magneto Resistance Effect."

The object of the work is briefly as follows:

- (1) To examine analytically and experimentally a new group of semiconductor devices based on the Hall-effect.
- (2) To study the feasibility of these devices in r.f. and microwave applications such as amplifiers, converters, and isolators.
- (3) To continue an experimental program on Tunnel Diode devices with special attention to
  - a) improved Tunnel Diodes
  - b) extend the operating frequencies of Tunnel Diode amplifiers and converters from the microwave to the millimeter wave region.

In recent years the solid-state microwave field has flourished through the use of such new devices as parametric and tunnel diodes. Their applications have not been free of problems, most of which are due to their negative impedance characteristic, combined with their two-terminal nature. Consequently, present thinking is being directed towards four-terminal active devices which operate at microwave frequencies. These devices should be non-reciprocal and have high-gain and low-noise properties. It is the scope of this contract to investigate a new group of such devices, whose operating principle is based on the Hall-effect.

Since the Hall-effect is a majority-carrier phenomenon it should have response to very high frequencies. Consequently, our work deals ultimately with the possibilities and limitations of incorporating this effect into new devices and microwave applications.

This investigation started with a study of a "low" frequency (2 mc) amplifier and converter to obtain a clearer understanding of the Hall-effect under actual operating conditions. An electronic gain of 43 db has been achieved, and thus evidence of the Hall-effect at high frequencies has been substantiated. However, although these results are promising, they are still not as high as the predictable theoretical values. One of the major



reasons for this limitation is in the deterioration of the  $\mu Q$  of the ferrite materials of the associated circuitry at more than a few hundred kilocycles.

Further experiments were carried out to utilize the Hall-effect in the conversion of frequency at the S-Band region of the microwave spectrum. The conversion gain which seemed to be feasible was found to be dependent on the control sensitivity of the conversion system. The present experimental model still suffered a conversion loss of 20 to 30 db. Special tests were performed by using a high-power pulsed microwave pump. Conversion gains were measured as a function of the pumping power and showed some "Saturation" effects. These effects were explored and explained on the basis of the behaviour of carriers in the sample under high power microwave fields. In particular, a breakdown field beyond which the saturation seemed to disappear was found.

Other schemes attempted an altogether different approach. Instead of relying solely on material characteristics for improved coupling efficiencies, they explore analytically and experimentally the possibilities of enhancing the interaction between the circuit and the Hall-effect device. While an enhanced effect under d.c. conditions was demonstrated before (see Final Report of Contract No. AF19(604)-4980), further studies and tests have been pursued to achieve similar results at microwave frequencies. This was done in a Hall amplifier at S-Band frequencies, in conjunction with a novel way of employing a single crystal yttrium iron garnet to improve the r.f. magnetic field coupling. The experimental results so far, have yielded a net gain of 2 db at a frequency of 3730 mc.

Several isolators based on the Hall-effect were built in a strip-line embodiment. They were designed and tested for a frequency of 0.6 Gc. Their semiconductor elements were mostly germanium wafers in the form of a rhombic geometry. These wafers carried multi-contact ports to reduce their forward insertion loss. With the maximum available d.c. magnetic field of 20K gauss an insertion loss of 5 db and an isolation of 8.5 db was obtained over a bandwidth of 140 mc.

Some time was spent on improving fabrication methods and technology of tunnel diodes for mm wave application. Of the three materials studied and tested under various parameters and conditions, gallium antimonide gave the best results.

A forward-biased tunnel diode, when used as a detector, is expected to be more sensitive than an ordinary crystal detector because of the greater non-linearity and lower series resistance. An improvement in sensitivity of 25 db as compared to an ordinary crystal detector has been obtained from a tunnel diode for an operation frequency of 55 Gc. An analysis indicates the non-linear capacitance contribution to sensitivity of a tunnel diode is negligible as compared to the non-linear resistance contribution.

## II. HALL-EFFECT DEVICES

### A. LOW FREQUENCY SCHEME

#### 1. *Description of Circuit*

As a starting point of our investigation, two basic Hall-effect circuits were built, namely an amplifier and a frequency converter, both operating with a signal frequency of 2 mc. A block and schematic diagram of the converter scheme are shown in Fig. 1 a, b, c. Fundamentally the circuit consisted of a semiconductor wafer to which an electric and a magnetic field were applied orthogonally. The input circuit (i.e. The signal circuit) was associated with the magnetic field, while the local oscillator provided the pump or control current through the sample. The output was obtained across the orthogonal terminals of the semiconductor at which the Hall voltage appeared. This arrangement was chosen because the signal voltage could be translated into the required magnetic field without unduly loading the signal source. This was accomplished by means of a ferrite ring into which a narrow gap had been cut. Sandwiched into this gap was the semiconductor wafer. The Signal Generator drove the primary coil of the input ferrite, while the secondary was tuned to resonance. The coupling between the two coils and the turns ratio were adjusted so that the input loop represented 50 ohms, and was matched to the Signal Generator impedance. The Local Oscillator was directly connected to the Hall sample because this yielded the maximum obtainable pump current, and matching was not critical. However, across the "output" terminals of the Hall sample matching was extremely important, and since the impedance across the sample was very low, a special transformer had to be provided to obtain resonant matching to the 50 ohm input of the i.f. amplifier.

The circuit for the Hall amplifier was quite similar, except that the Local Oscillator was replaced by a d.c. pump source, and the output impedance was matched into a sensitive r.f. receiver at the signal frequency instead of the i.f. frequency. Special precautions had to be taken, however, to eliminate any undesirable direct coupling between the input and output circuit. Through careful construction layout the stray pick-ups due to the ferrites and the associated wiring were successfully minimized. Another problem which arose due to the inductive coupling of the output loop to the magnetic field of the gap in the input ferrite was eliminated by means of a bucking loop. This resulted in an effective isolation of 60 db between input and output terminals.

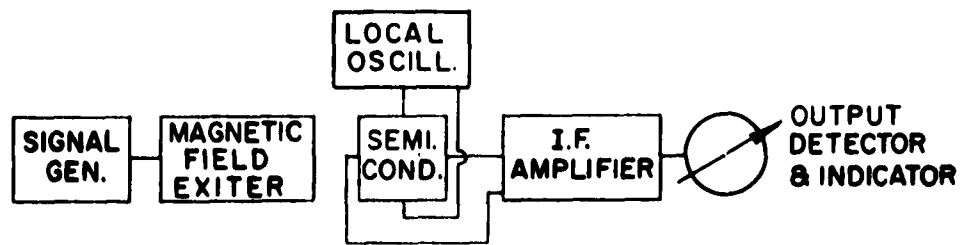


FIG. 1a

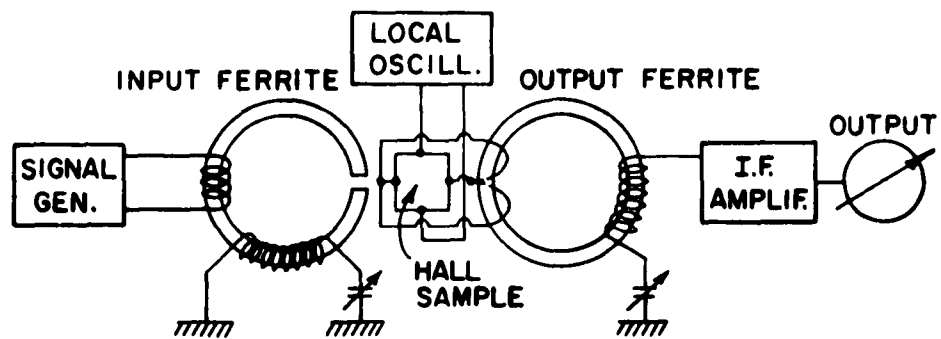


FIG. 1b

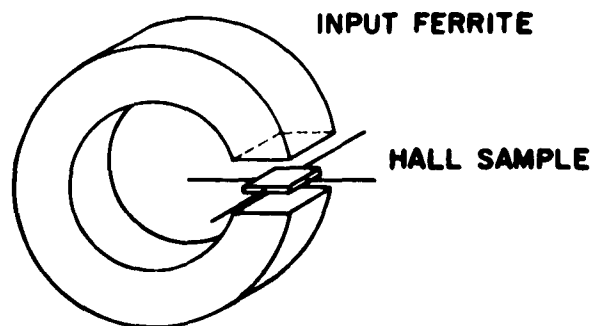


FIG. 1c

**BLOCK AND SCHEMATIC DIAGRAM OF HALL EFFECT CONVERTER**

## 2. Construction of Device

In designing the Hall-effect amplifier a principal consideration had to be given to the choice of material for the Hall sample itself. The analytical expression for the power gain clearly showed that the most important material characteristic was that of the Hall mobility. This then dictated the choice of Indium Antimonide, which has the highest mobility of all presently available semiconductors. The material used in our experiments was n-type, single crystal InSb with the following characteristics measured at room temperature and at liquid nitrogen respectively:

	$T = 300^{\circ}K$	$T = 78^{\circ}K$
$N \text{ (cm}^{-3}\text{)}$	$1.8 \times 10^{16}$	$7.5 \times 10^{13}$
$R_H \text{ (cm}^3\text{coulomb}^{-1}\text{)}$	340	$8.3 \times 10^4$
$\rho(H=0), \text{ (ohm-cm)}$	0.005	0.18
$\mu \text{ (cm}^2\text{vol}^{-1}\text{sec}^{-1}\text{)}$	$6.8 \times 10^4$	$4.6 \times 10^5$

It followed that in order to obtain highest amplification the coupling of the r.f. magnetic field to the Hall sample had to be as high as possible. This then resulted in definite requirements for the choice of the ferrite material and its construction. The advantage of using a ferrite material lies in the magnetic flux concentration that can be obtained near the sample and therefore depended on the ferrite's magnetic permeability  $\mu_m$ , and loss factor  $Q$  at the frequency of operation. At the beginning of our experiments we used a special ferrite produced at the RCA Laboratories which had a  $\mu_m \approx 200$  and an unloaded  $Q \approx 100$  at a frequency of 2 mc. The resultant  $\mu Q$  product of 20,000 is one of the highest presently available at this frequency.

In order to maintain the magnetic flux density as high as possible it became necessary to make the air gap in the ferrite as small as possible. This requirement imposed considerable difficulties on the preparation of the semiconductor sample, which had to fit into such a small gap, because InSb is a very brittle material. The first samples were prepared from wafers .060" x .060" with a thickness of .003". To facilitate their handling and to give support to the solder contacts at the edge of the specimen, the assemblies were placed on ceramic substrates of .010" thickness. Thus a gap of at least .015" was required to accommodate the packaged assembly.

Subsequently an improved technique was used that permitted a much smaller gap width. In this technique a semiconductor wafer was cemented to a substrate made of the

same ferrite material used for the input ferrite. These ferrites had a very high electrical resistivity and therefore did not cause any by-passing to the sample. After making the necessary solder connections to the sample, the assembly was encased in araldite and then lapped down until the InSb wafer was less than .001" in thickness. Another piece of ferrite (similar to the first one) was then cemented on top of the sample and finally the whole assembly was placed into the gap of the input ferrite. While the whole ferrite - InSb - ferrite sandwich was approximately .060" thick, and therefore gave no problem in handling, the effective gap in the ferrite was only the thickness of the InSb, namely .001".

### **3. Experimental Results and Discussion**

As mentioned before our first efforts were concentrated on the converter circuit. During the course of the experiment it was noted that the output was increased when a magnetic field produced by a small permanent magnet was added to the magnetic field excited by the signal. This permanent magnetic "bias" field could be adjusted to a critical value, at which the net conversion power ratio became almost unity. Further investigation showed that this improvement was not caused by an increase in Hall-effect voltage alone, but also by the secondary effect of strong non-linearity in the magnetization curve of the ferrite at the point of critical permanent field biasing. This non-linearity in connection with a large pump current caused an undesirable parametric conversion, which was not in line with the objective of the present investigation. Consequently, it was decided to put the converter circuit temporarily in abeyance, and continue with efforts on the Hall-effect amplifier.

The results achieved with the Hall-effect amplifier at an operating frequency of 2 mc are quite promising but have not yet attained the predictable theoretical values. With the previously described Hall sample of 3 mils thickness and an air gap of 15 mils in the magnetic circuit of electronic gain of 30 db was obtained when the sample was pumped with 500 ma d.c. current.

Further tests with a new sample made by the improved fabrication technique gave an increase in electronic gain to 43 db. Because of the extreme thinness of the sample (only 0.7 mils) the test was made under pulsed pump conditions with a low duty cycle. Since the input-to-output isolation of this amplifier was 60 db when the circuit was optimized for sensitivity, there still remained a net loss of 17 db.

Theoretical calculations show that such gain limitations are not basic for these Hall amplifiers, but rather are caused by the low efficiency of the particular embodiment,

and the materials involved. Several tests are still in progress to determine the cause of this discrepancy.

One of the prime reasons is the low coupling efficiency of the signal via the magnetic field of the ferrite to the sample. The state of the art in ferrite technology is limiting the  $\mu Q$  product of these materials quite severely in frequencies above a few hundred kilocycles. Several materials from various sources have been tried, because they showed promising characteristics at least in one of the two factors. But unfortunately they always also showed marked deficiencies in the other factor. The  $\mu Q$  product of our originally chosen ferrite material is still, relatively speaking, the best available yet.

Of further importance seems to be the effect that the current electrodes of the Hall sample have, because they tend to short-circuit the developed Hall voltage. Small, multiple current electrodes, properly insulated from one another, are being prepared to replace the large, single-current electrode formerly used.

Other tests have been initiated to probe into the quantitative behavior of the Hall mobility with decreasing semiconductor thickness. While an extremely thin sample is required to obtain useful gain, it has been suspected that the mobility of the sample went down rapidly as the sample thickness decreased. It has been known that the Hall-effect and magneto-resistance are strongly dependent on surface states, but further quantitative data were needed. Therefore an investigation has been started to establish the relationship between mobility and sample thickness of variously treated surfaces. While this investigation is by no means completed, the tests so far have shown that the thickness of the sample can be reduced to 3 mils before a drastic reduction of mobility is noticed. Above 3 mils the mobility of the sample stayed practically constant at its "bulk" value of  $6.3 \times 10^4 \text{ cm}^2 \text{ volt}^{-1} \text{ sec}^{-1}$  (for the single crystal n-type InSb). Within the observed range of thickness (i.e. from 30 to 3 mils) it did not seem to make any difference whether the sample thickness was reduced by lapping with a 3 micron abrasive, or by chemical etching. Below 3 mils thickness the sample was of necessity etched only, but even with this precaution the mobility dropped to 50% of its bulk value when the sample thickness had reached 1 mil.

Summing up the latest results of the low frequency study, a clearer understanding of the complexities of the Hall-effect amplifier has been gained. Evidence of the effect at high frequencies has been substantiated, its dependence on high mobility materials has been verified. Cooling of the semiconductor has shown that the a.f. impedance of the sample increases in the same manner as its d.c. resistance, thus producing a 20 db improvement in the obtainable output. The device could easily be followed by a tunnel diode to give further gain per stage.

While the above-mentioned tests have revealed the possibilities of Hall-effect amplifiers, they have also shown the limitations imposed by the associated circuitry and materials. This is most noticable in the limited  $\mu Q$  range of the ferrite materials as higher frequencies are approached. Consequently, new solutions to this problem must be investigated. Several worthwhile ideas have been proposed.

The first one of these proposals deals with a Hall-effect converter in the S-Band region of the microwave spectrum. To improve the coupling between the Hall sample and the r.f. magnetic field of the driving microwave cavity, a material of high dielectric constant (such as rutile) is placed in the cavity next to the sample. This should concentrate the r.f. magnetic field in the vicinity of the sample and thereby improve the coupling. The second proposal is similar in nature, and seeks an improved coupling in a Hall-effect micro-amplifier by means of a novel way of employing a single crystal yttrium iron garnet (YIG). The improved coupling was combined with an attempt of an altogether different approach. Instead of relying solely on material characteristics for improved coupling efficiencies, the possibilities of enhancing the interaction between the circuit and the Hall-effect device were explored analytically and experimentally.

## **B. MICROWAVE CONVERTERS**

### **1. Introduction**

The aim of the present work was to investigate the utilization of the Hall-effect in the frequency conversion of microwaves, and in particular, to determine the limiting values of the obtainable sensitivity and possible gain. Frequency conversion based on the Hall-effect has been known for some time. However, the Hall converter investigated here was different from previously described devices<sup>(1,2)</sup> in several respects. The present scheme used a magnetic field at the signal frequency ( $f_s$ ) to interact in a Hall sample with an electric field supplied by a large pump source of frequency ( $f_p$ ). The resultant Hall voltage contained the desired difference frequency ( $f_s - f_p$ ). This arrangement has the characteristics of an active device, with the conversion gain dependent on the control sensitivity of the device. A high control sensitivity seemed feasible through the use of a high-mobility

---

(1) B. R. Russell and C. Wahlig, Rev. Sci. Instr. 21, 1028 (1950).

(2) H. E. M. Barlow, K. V. G. Krishna, British I.E.E. 131 (1961).

Hall sample, efficient coupling of the modulating magnetic field to the sample, and a suitable high energy pump source. It was the purpose of this investigation to explore how well these three requirements could be met.

To satisfy the first one, InSb, a IV-V semiconducting compound, well known for its high electron mobility was chosen for the Hall sample. The fulfillment of the second requirement was sought by means of a microwave cavity, and by locating the sample at a point of highly concentrated r.f. magnetic field. The third requirement, i.e., to provide a high electrical field in the sample, involved some special problems, because of "saturation" effects in the semiconductor. A considerable effort was made to explore and explain these effects stemming from the behaviour of carriers under high power microwave fields. This phase of the experiments was of particular interest, since it combined the Hall-effect at microwave frequencies with high electrical fields, thus going beyond the scope of the previous investigations.<sup>(3,4,5)</sup> The results were encouraging and promised the feasibility of a high-gain amplifier at very high power levels.

## **2. Experimental Hall-Effect Converter**

The microwave cavity used for the study of the Hall-effect converter is shown in Fig. 2. A reentrant coaxial cavity was used. A disk-shaped InSb sample about .005" thick and .200" in diameter was mounted at the reentrant post. The reentrant gap was filled with another disk made of high dielectric constant material, such as rutile. The purpose of this dielectric disk was to concentrate the r.f. magnetic field in the vicinity of the sample so that coupling to the field could be achieved in a highly efficient way. Both the input signal and the pump were applied to the cavity through the coupling loop. The output r.f. signal, whose frequency is the difference of the signal frequency and the pump frequency, was derived through the Hall-effect and fed to the coaxial line.

The reentrant cavity is characterized by a high r.f. field concentration near the post where the sample is mounted. The signal has an azimuthal magnetic field  $B$  around the sample which is used to modulate the axial field  $E_z$  due to the pump. The resulting Hall field was then produced radially in the sample. The r.f. field near the post is expected to be non-uniform. For the purpose of simple physical reasoning, an average uniform field was assumed to exist in the sample. In addition, the sample was designed to be thinner than the skin depth.

---

(3) J. B. Gunn, J. Electronics 2, 87 (1956).

(4) M. Glicksman and M. C. Steele, Phys. Rev. 110, 1024 (1958).

(5) K. Rose, J. Appl. Phys. 33, 761 (1962).



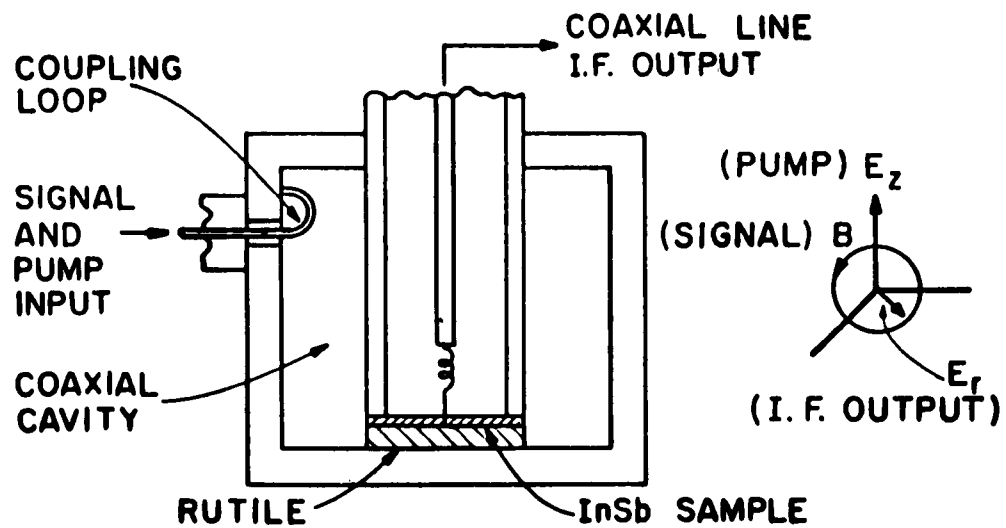


FIG. 2. HALL-EFFECT MICROWAVE CONVERTER.

The experiments were performed mostly at 77°K, liquid nitrogen temperature. The cavity was vacuum sealed into a metallic container, which was cooled in a Dewar flask filled with liquid nitrogen.

### 3. Experimental Results

The InSb samples used for the measurement were of single crystals, n-type doped. Typical electrical parameters of these crystals at 77°K are as follows:

Electron Mobility	$(3 - 5) \times 10^5 \text{ cm}^2 \text{ V}^{-1} \text{ sec}^{-1}$
Resistivity	0.1 - 0.4 Ohm-cm
Net carrier concentration	$(0.5 - 2) \times 10^{14} \text{ cm}^{-3}$

A number of InSb samples made from the same material and with the same dimensions were tested and only a few samples yielded reproducible results. These results are shown in Fig. 3. The solid curves show the experimental electronic gain vs frequency plot of five samples. Since each sample is sandwiched between the rutile and the cavity post, and because the rutile has a much higher dielectric constant than the InSb, the resonant frequency is expected to change in a very sensitive way with the dimensions and electric parameters of the InSb sample. This change in resonant frequency for five samples presumably made of same dimensions and material is shown in Fig. 3. The circuit Q of the cavity was measured to be 60. The pump frequency was about 4 mc higher than the incoming signal frequency so that a 4 mc output signal was obtained as the intermediate frequency.

The converter was evaluated in terms of electronic conversion gain, which is defined as the ratio of the power output at i.f. to the available power input at signal frequency. The largest reproducible net gain as shown by Fig. 3 was -24 db and the corresponding bandwidth was of the order of 50 mc. Once a net gain as high as -17 db was observed but it was not reproducible.

The above results were obtained with a moderate pump power of the order of 200 milliwatts. It was felt that the use of higher pumping powers might lead to some improvement in gain. The high-power test was performed by using a pulsed microwave pump, a pulsed traveling-wave tube which was capable of delivering a 50 W peak power at S-band with a pulse width of 1  $\mu$ sec and a repetition rate of 1000 cycles.

A run of i.f. power versus pumping power was attempted on one of the InSb samples. Results are shown in Fig. 4. I.F. powers were normalized at the 30 watt peak level.

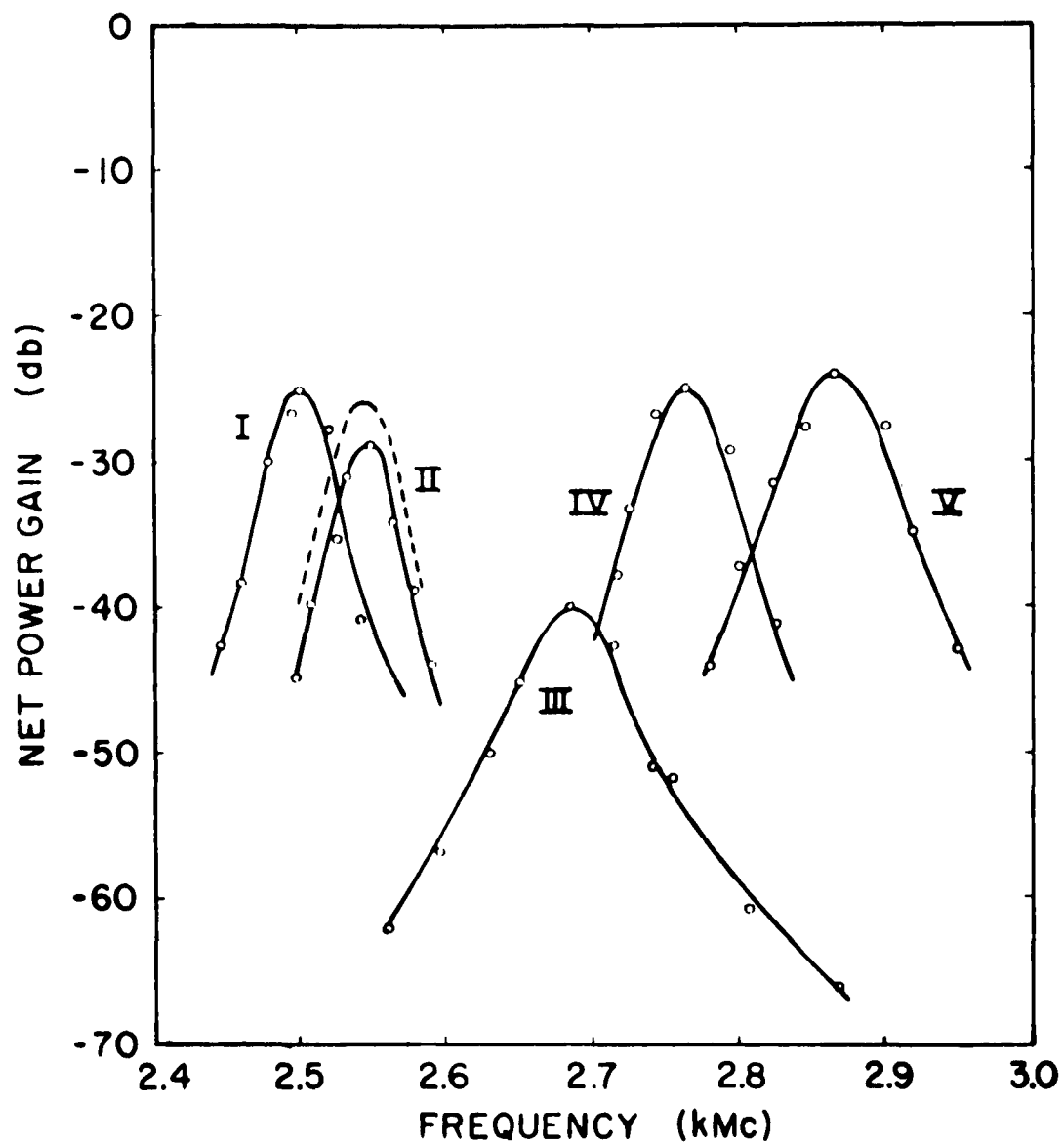


**FIG. 3.** CONVERSION POWER GAIN EXHIBITED BY FIVE InSb SAMPLES.

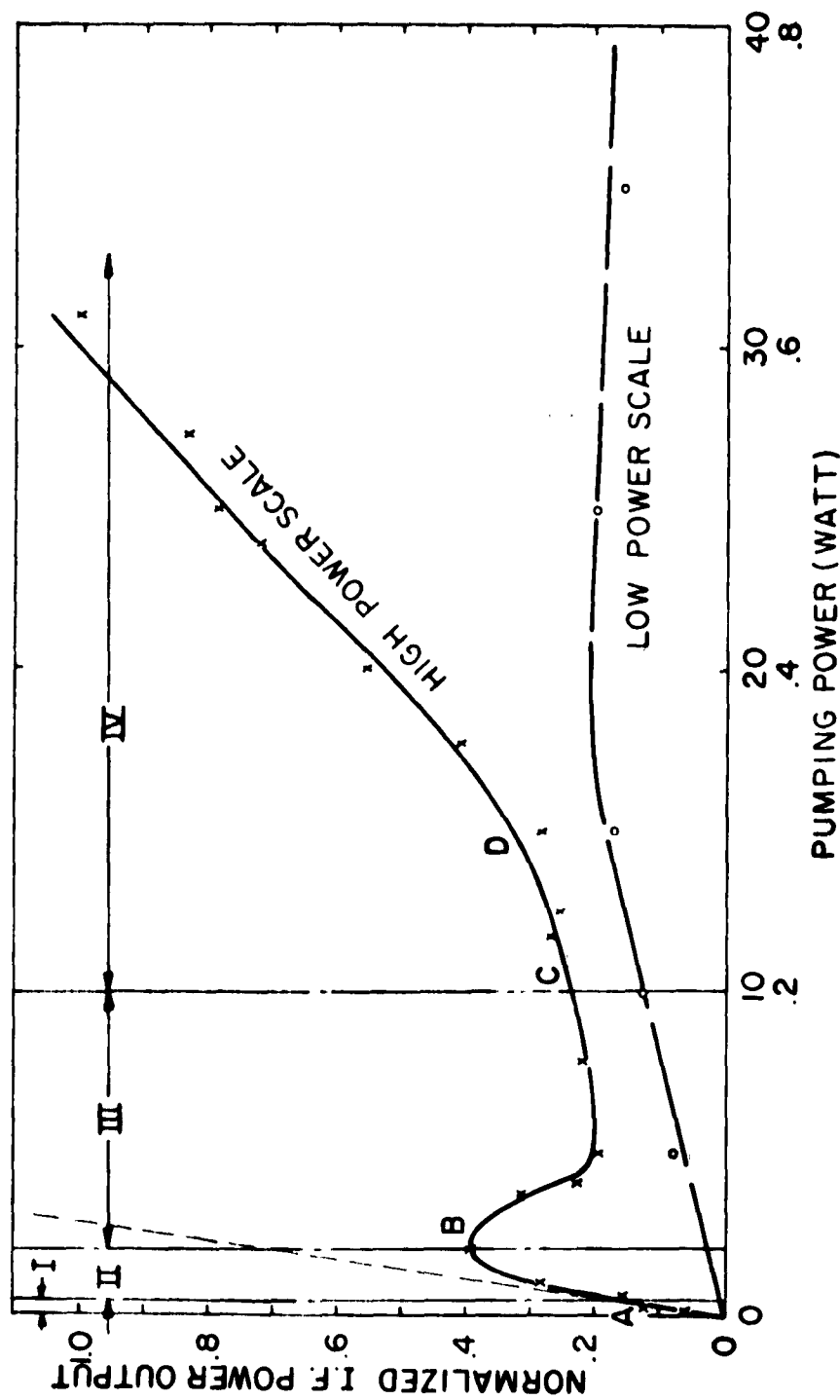


**FIG. 4.** I.F. POWER OUTPUT AT HIGH PUMPING FIELDS

The solid curve gives the experimental results. Had the mobility and the conductivity been independent of the electric field, the i.f. output power would have varied linearly with the pumping power. This idealized i.f. power is shown by a dotted line. At very small pump powers, the experimental i.f. powers followed the idealized one. As the pumping power became larger, the measured power deviated more and more from the idealized value. The i.f. power first reached a peak point at the 2 watt level, then dropped to a valley point at the 6 watt level and finally increased again almost linearly with respect to the pumping power.

#### 4. Discussion

The output Hall field which results from the modulation of the magnetic field is

$$E_o = \frac{RJ B}{2} = \left( \frac{\mu}{\sigma} \right) \frac{\sigma E}{2} B = \frac{\mu B}{2} E \quad (1)$$

where  $E_o$  - Output Hall-field  
 $R$  - Hall coefficient  
 $J$  = Pumping current density  
 $B$  = Modulating magnetic field  
 $\mu$  - Mobility of the sample  
 $\sigma$  - Conductivity of the sample  
 $E$  = Pumping electric field

The factor  $(\frac{1}{2})$  in the output field arises from the cross product of the pumping electric field and the modulating magnetic field at two different frequencies.

The conversion power gain can be shown to be equal to

$$G_p = \frac{\mu^2}{a^2} P_o \frac{g g_L}{(g_L + g)^2} R_g \quad (2)$$

where  $a$  is a constant with the dimension of velocity so that  $aB$  has the dimensions of field. In practice,  $aB$  is the input signal field applied to the circuit which produces the modulating field.  $P_o$  is the applied pumping power.  $g$  is the conductance of the sample in the output circuit,  $g_L$  is the load conductance, and  $R_g$  is the signal generator internal resistance.

To estimate the value of  $a$  for the experimental Hall converter, assume most of the microwave field to be concentrated uniformly in the sample near the post. It then follows that<sup>(6)</sup>

$$a = \sqrt{\frac{2\omega\tau R_g}{\mu_o R}} \quad (3)$$

where  $\omega$  is the resonant frequency,  $\tau$  is the volume of the sample,  $\mu_o$  is the permeability of air and  $Q$  is the quality factor of the cavity. For the present circuit configuration of  $Q = 50$  with an InSb sample of mobility of the order of  $500,000 \text{ cm}^2 \text{ V}^{-1} \text{ sec}^{-1}$  and dimensions of .200" diameter and .005" thickness, the computed conversion power gain of sample II is about -28 db. This computed gain is also shown in Fig. 3 by a dashed curve, which is in good agreement with the measured one.

In principle, the Hall converter is an active device. It should yield conversion gain with a suitable pump supply. However, the proto-type experimental model has not achieved a net gain and has suffered a conversion loss of 20 to 30 db. This loss is probably due to two reasons. The sample is too large in dimensions to have adequate microwave energy penetration and the coupling between the sample and the r.f. field is inefficient for the particular configuration in question. As given by the gain expression, the gain is inversely proportional to the volume of the cavity. A smaller cavity should improve the coupling. The present cavity is by no means an optimized one, since the magnetic field is localized only at the edge of the post. As a result, the sample at the center of the post does not intercept the full magnetic field.

The purpose of the high-power experiment was to explore the limitation of the Hall-effect at high fields in InSb at microwave frequencies. It is a well known fact that the departure from Ohm's law on bulk semiconductors in high electric fields is due to the dependency of the mobility on the applied field. Electrons travel in the crystal with a drift velocity which is proportional to the applied field when the field is small. As the field becomes high, the electron energy increases because the loss of its excess energy due to scattering becomes inefficient in maintaining thermal equilibrium. In most cases, the electrons have a reduced drift velocity as their energy increases. As a result, the linear relationship between the drift velocity and the applied field no longer holds. In a moderate field, the mobility due to lattice scattering is given as<sup>(7)</sup>

(6) A. B. Boonwell and R. E. Beam, *Theory and Application of Microwaves*, McGraw-Hill Book Company, Inc., 1947.

(7) R. A. Smith, *Semiconductors*, Cambridge University Press 160-162, (1959).

$$\mu_1 = \mu_o \left[ 1 - \frac{3 \pi \mu_o^2}{64 u^2} E^2 \right] \quad (4)$$

where  $\mu_o$  is the small-field mobility,  $u$  is the velocity of sound in the crystal and  $E$  is the applied field. A moderate field means  $E \ll \frac{u}{\mu_o}$ .

As  $E$  is increased so that  $E \gg \frac{u}{\mu_o}$  the mobility becomes<sup>(7)</sup>

$$\mu_2 = (32/3\pi)^{1/4} (\mu_o u)^{1/2} E^{-1/2} \quad (5)$$

In a very high field in which the drift velocity of electrons reaches a value comparable with an energy  $\hbar\eta_o$ , where  $\eta_o$  is the frequency corresponding to the optical modes, these modes are excited and a large fraction of the kinetic energy of an electron is absorbed by these optical modes. The mobility resulting from this interaction can be shown<sup>(7)</sup> to be equal to

$$\mu_3 = \frac{e}{m} (r_o) = \left( \frac{\hbar\eta_o}{m_e} \right)^{1/2} E^{-1} \quad (6)$$

Both the drift velocity and the current density saturate under this condition.

The change of mobility of InSb under the influence of a high field has been substantiated at microwave frequencies in the present Hall converter. Evidence of a drop in mobility in high fields is indicated in Fig. 4. The gain equation can be expressed in terms of mobility as follows:

$$(G_p)_I \approx \mu^3 \frac{P_o}{\left( 1 + \frac{g_o}{g_L} \frac{u}{\mu_o} \right)^2} \quad (7)$$

To interpret the experimental curves shown by Fig. 4, separate the curve into four regions. In region I, where the field is small,  $G_p$  varies as  $P_o$  and the mobility follows  $\mu$ , which is almost a constant. The field at the point A is about 10 volt/cm which is large compared to  $\frac{u}{\mu_o} \approx 1$  volt/cm. Thus the region beyond A which is designated by II, should use  $\mu_2$  in computing the gain. This gain is

$$(G_p)_{II} \approx P_o^{1/4} \quad (8)$$

(7) R. A. Smith, Semiconductors, Cambridge University Press 160-162, (1959).

which explains the non-linear relationship with respect to the pump power in the region II.

As the pump power is further increased, electrons in the crystal reach drift velocities which excite the optical modes. Using the mobility  $\mu_3$ , the gain resulting from this interaction can be shown to be

$$(G_p)_{III} \approx \frac{1}{(P + I_s^2/g_L)^2} \quad (9)$$

where  $I_s$  is the saturation current which would flow in the sample under a high field for optical-mode scattering. Thus the gain varies inversely as the square of the pump power. This trend is strongly indicated by the curve *BC* in region III.

Then the question arises as to why the gain increases again beyond the point *C*, which is marked by region IV. This is the region which marks the onset of a new phenomenon interpreted as an avalanche breakdown. The process involves a sudden increase in the number of carriers which hitherto has been assumed to be constant. Hole-electron pairs are created. The minimum energy which an electron must possess to produce such a pair must be greater than the forbidden energy gap of the semiconductor. The estimated field in the sample at the point *D* is of the order of 400 volts/cm, which is well in the breakdown region for InSb according to previously published results.<sup>(4)</sup>

## 5. Conclusions

Experiments on a prototype microwave Hall-effect frequency converter have led to the following conclusions:

(1) While the present experimental model still suffers a conversion loss of 20 to 30 db, results have revealed that a microwave Hall converter with gain should be possible. Such a converter should be designed with a thin semiconductor sample of high mobility of the order of  $500,000 \text{ cm}^2\text{V}^{-1}\text{sec}^{-1}$ , and a cavity which offers both a loaded *Q* and a field coupling to the sample one order of magnitude higher than the present cavity, as well as a suitable high-power pulsed pump.

(2) By using the avalanche ionization, it is possible that the device will yield gains which increase with pump powers at very high pumping fields. The range of power handling capacity of the proposed amplifier should be good, and should not be limited by small pump power restrictions. This is an advantage of the large pump power requirement expected for operation in the avalanche mode.



(3) The Hall-effect device operates with majority carriers. The only noise involved is the Johnson noise. Thus the noise can be reduced by cooling. It is conceivable that under this condition the Hall converter will turn out to be a low-noise device.

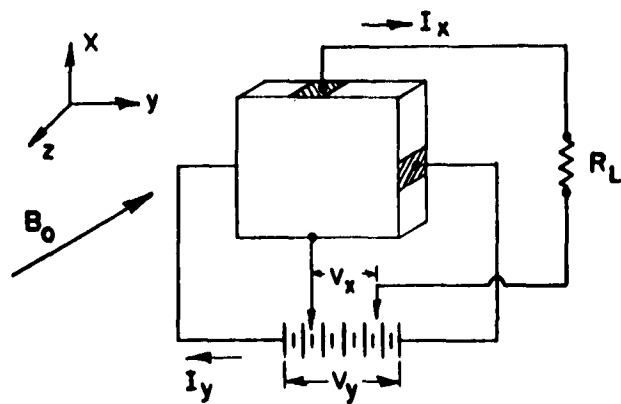
## C. ENHANCED HALL-EFFECT AMPLIFIER

### 1. Introduction

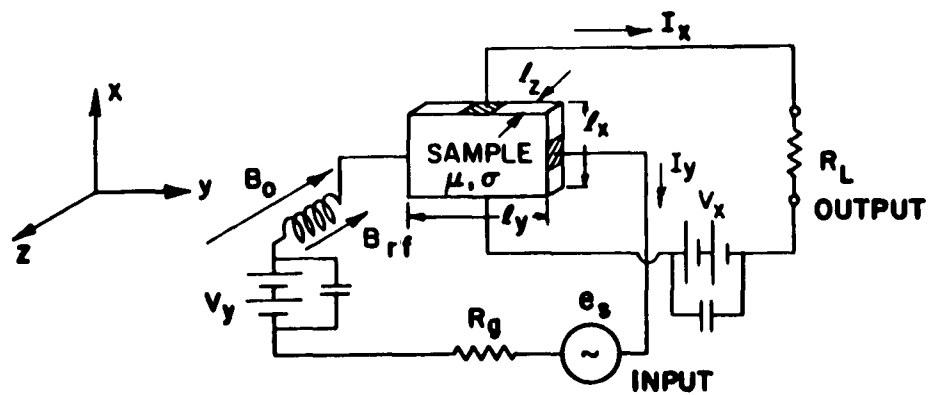
In the past, Hall-effect devices have been built at audio frequencies. Because of their inefficient operation, high frequency applications have not been possible. To improve the efficiency of the Hall-effect interaction an enhanced amplifier scheme was proposed. Figure 5a shows its d.c. model. The scheme consists of supplying to a semiconductor wafer a longitudinal electric field (from battery  $V_x$ ), and a transverse current ( $I_y$  from battery  $V_y$ ), both from a common source. The fact that  $V_x$  and  $V_y$  are from a common source simply implies that they vary together in a given relationship. In addition, an orthogonal magnetic field ( $B_o$ ) is applied to the semiconductor sample, such that the resulting Hall field ( $\approx I_y \times B_o$ ) opposes the applied longitudinal electric field. Thus if the Hall field and the applied field are varied together the current in the longitudinal direction changes little and the impedance is, in effect, high. However, a change in the magnetic field upsets the balance so that the longitudinal current becomes very sensitive to the magnetic field. This enhanced Hall-effect has been substantiated in a simultaneous d.c. measurement of magnetic resistance and Hall-effect on a semiconductor sample.

### 2. R.F. Amplifier Model

Recently a practical r.f. model has been conceived. Figure 5b shows the r.f. model.  $V_x$  and  $V_y$  are the d.c. batteries which are the energy supplies for the device. The input circuit supplies the magnetic field for modulation, as well as delivers r.f. energy to the sample. The use of the input r.f. energy is found necessary for producing the enhanced effect. As a corollary to the d.c. model we find the r.f. Hall field due to the product of the r.f. current  $\hat{I}_y$  and the steady state magnetic field  $B_o$ ; furthermore, the longitudinal r.f. field  $\hat{V}_x$  as the product of the d.c. current  $I_x$  or  $I_y$  and the r.f. magnetic field  $B_{rf}$  and finally the r.f. transverse current simply as the r.f. current  $\hat{I}_y$ . Just as  $\hat{V}_x$  and  $\hat{I}_y$  in the d.c. model are controlled from a common source, so are  $V_x$  and  $I_y$  in the r.f. model, namely from the common r.f. signal source  $e_s$ . It can also be shown that the device has perfect isolation provided certain relations between the circuit and sample parameters are satisfied.



D.C. MODEL OF ENHANCED HALL -EFFECT AMPLIFIER  
FIG. 5a



R.F. MODEL OF ENHANCED HALL -EFFECT AMPLIFIER  
FIG. 5b

### 3. Analysis of r.f. Amplifier Model

The static d.c. current-voltage equations are:

$$I_x = \frac{g_x V_x - g_y V_y \theta (\ell_y / \ell_x)}{1 + \theta^2} \quad (10)$$

$$I_y = \frac{g_x V_y + g_y V_x \theta (\ell_x / \ell_y)}{1 + \theta^2} \quad (11)$$

where  $\theta = \mu B_0$ , the Hall angle in radians equal to the product of the mobility and the magnetic field.

Small-signal equations can be written as

$$\hat{I}_x = g_{xc} e_s + g_{xx} \hat{V}_x + g_{xy} \hat{V}_y \quad (12)$$

$$g_g e_s = g_{yc} e_s + (g_{yy} + g_g) \hat{V}_y + g_{yx} \hat{V}_x \quad (13)$$

where

$$g_{xc} = a\mu [g_x V_x (2\theta) - g_y V_y (\theta^2 - 1) \ell_y / \ell_x] (1 + \theta^2)^{-2} \quad (14)$$

$$g_{yc} = a\mu [g_y V_y (2\theta) + g_x V_x (\theta^2 - 1) \ell_x / \ell_y] (1 + \theta^2)^{-2} \quad (15)$$

$$g_{xx} = \frac{g_x}{1 + \theta^2} \quad (16)$$

$$g_{yy} = \frac{g_y}{1 + \theta^2} \quad (17)$$

$$g_{xy} = \frac{-g_y \theta}{1 + \theta^2} (\ell_y / \ell_x) \quad (18)$$

$$g_{yx} = \frac{g_x \theta}{1 + \theta^2} (\ell_x / \ell_y) \quad (19)$$

where  $a = \frac{B_r I}{c_s}$

On solving 12 and 13 simultaneously, one obtains

$$\hat{V}_x = - \frac{g_{xc}(g_{yy} + g_g) - g_{xy}(g_{yc} + g_g)}{(g_{xx} + g_L)(g_{yy} + g_g) - g_{xy}g_{yx}} e_x \quad (20)$$

$$\hat{V}_y = - \frac{(g_{yc} + g_g)(g_{xx} + g_L) - g_{xc}g_{yx}}{(g_{xx} + g_L)(g_{yy} + g_g) - g_{xy}g_{yx}} e_s \quad (21)$$

$\hat{V}_y$  is a function of the output conductance  $g_L$ . The dependency can be removed by properly choosing  $g_L$ . To do this, let

$$g_L = - \frac{l_y}{l_x} \frac{1}{\theta} \left( \frac{g_g + g_y}{g_g + g_{yc}} \right) g_{xc} \quad (22)$$

Equations 20 and 21 then become

$$\hat{V}_x = \frac{-g_{xy}}{g_{xx}} \frac{(g_{yc} + g_g)}{(g_g + g_y)} e_s \quad (23)$$

$$\hat{V}_y = \frac{(-g_{yc} + g_g)}{(g_g + g_y)} e_s \quad (24)$$

#### 4. Power Gain

$$G_p = \frac{4g_{xc}}{rg_g} \frac{l_x}{l_y} \theta = \frac{4}{r} a\mu \sqrt{P_m g_y} \theta R_g \quad (25)$$

where

$$P_m = \frac{1}{(1 + \theta^2)^4} [P_x(4\theta^2) - 4\sqrt{P_x P_y}(\theta^2 - 1) + P_y(\theta^2 - 1)] \quad (26)$$

$$P_x = V_x^2 g_x \quad P_y = V_y^2 g_y \quad r = \frac{g_g + g_y}{g_g - g_{yc}}$$

$P$ 's being the d.c. input powers.

The power gain for a conventional Hall amplifier where there is no enhanced effect is

$$G_p' = a^2 \mu^2 \frac{P_m}{g_g} (1 + \theta^2) \quad (27)$$

Ratios of  $G_p$  to  $G_p'$  for different d.c. magnetic fields are listed in Table I. The load resistance chosen for the enhanced amplifier is

$$R_L = \frac{\ell_x}{2\ell_y} \theta \frac{1}{g_{xc}} \quad (28)$$

Which is derived from 22 by assuming  $g_g = g_y$  and  $g_g \gg g_{yc}$ . This is the case when the input generator is matched to the sample and the sample conductance is high. By 25, a high sample conductance is required for a high power gain.

TABLE I

	CASE I High - d.c. magnetic field $\theta \gg 1$	CASE II Average - d.c. magnetic field $\theta = 1$	CASE III Low - d.c. magnetic field $\theta < 1$
$G_p$	$\frac{4}{r} a \mu \sqrt{P_m g_y} \theta R_g$	$\frac{4}{r} a \mu \sqrt{P_m g_y} R_g$	$\frac{4}{r} a \mu \sqrt{P_m g_y} \theta R_g$
$G_p'$	$a^2 \mu^2 P_m R_g (1 + \theta^2)$	$2 a^2 \mu^2 P_m R_g$	$a^2 \mu^2 P_m R_g$
$\frac{G_p}{G_p'}$	$\frac{4 \sqrt{g_y} \theta}{r a \mu \sqrt{P_m} (1 + \theta^2)}$	$\frac{2 \sqrt{g_y}}{r a \mu \sqrt{P_m}}$	$\frac{4 \sqrt{g_y}}{r a \mu \sqrt{P_m}} \theta$

## 5. Discussion

The ratio  $G_p/G_p'$  in Table I would numerically define the magnitude of the enhanced effect of the new Hall amplifier. The larger this ratio, the more pronounced is the effect.

Large enhanced effect is noticed at high d.c. magnetic fields with reduced power gains. It is interesting to note that  $G_p/G_p'$  varies as the square root of  $g_y$ , the sample conductance in the input circuit which produces the Hall field responsible for the enhancement. With a sample of a given conductivity,  $g_y$  is determined by the geometry of the sample. Therefore, through geometric optimization, samples of large enhanced effect can be fabricated and amplifiers of high gains can be realized.

## **6. Experimental Setup**

In order to demonstrate the enhanced Hall-effect amplifier a microwave amplifier was built. This embodiment also used a novel way of improvising the magnetic field coupling.

In recent years a ferrite-like material in the form of yttrium iron garnet (YIG) has been made available which operates at microwave frequencies. In our experimental setup it was used to concentrate the r.f. magnetic field in the vicinity of the Hall-effect sample, thereby improving the coupling of the input to the sample.

YIG materials presently known have high unloaded  $Q$ 's for a frequency range from 2 Gc to several Gc. YIG structures usually employ crossed coaxial transmission lines or crossed loops. A crossed coupling structure is required for the effective use of the interaction of the input r.f. magnetic field and the d.c. magnetic field. In the absence of the d.c. magnetic field there is practically no coupling between the r.f. field of the input line to that of the output line. Only when the d.c. magnetic field is present will r.f. energy be transferred from the input to the output. The insertion loss (in the presence of the d.c. magnetic field) is very low, usually .5 to 1.5 db per resonant stage. Without the d.c. field the insertion loss is very high, generally about 40 db. In addition to the control of the coupling, the d.c. field also determines the frequency at which the YIG resonates. This makes it possible to tune a YIG resonator by simply varying the d.c. magnetic field.

Our experimental circuit consisted of two concentric, short-circuited transmission lines which were orthogonal to each other. One served as input, the other as output. They crossed each other near their shorted ends, and it was at this point that the YIG was placed between them. This put the YIG near a place where the r.f. magnetic field reaches its maximum. The Hall sample, made of single crystal n-type Indium Antimonide was placed very close to the YIG sphere, to take full advantage of the highly concentrated r.f. magnetic field near the surface of the YIG. By this geometric arrangement, it was also intended to obtain the enhanced effect according to the above-mentioned theory. The experimental results so far have yielded a net gain of 2 db at a frequency of 3730 mc. While these preliminary results

have been encouraging, it is felt that further improvement can be made. Work is in progress to obtain better matching between the YIG circuitry and the sample circuitry.

#### **D. ISOLATOR**

An isolator employing a germanium crystal in strip line embodiment was constructed and tested. The following is a summary of the experimental data obtained for this isolator: input impedance as seen from either port, 50 ohms, voltage standing wave ratio, less than 1.3 over the frequency band of 560-680 mc/s; forward insertion loss of about 17 dbs and backward insertion loss of between 38 dbs and 45 dbs over the same frequency band. Thus isolation of better than 21 dbs over the passband was observed at an imposed external magnetic field strength of about 9500 Gauss. Although the forward insertion loss measured (17 dbs) was rather high, and this, by the way, was the only undesirable feature of the above isolator, it is, however, an expected quantity for low mobility germanium crystals immersed in magnetic field strengths of the order of magnitude quoted previously.

The work was then continued with main emphasis placed on the high-efficiency or small-insertion-loss multicontact case. An isolator employing a Germanium crystal and carrying six pairs of contacts per port (twenty four contacts altogether placed around its edges) was constructed in strip line and was briefly tested. The following results were obtained (no optimization was again attempted) over the frequency band 500-640 mc: forward insertion loss, 10 db, backward insertion loss, varying between 35 and 55 db, thus an isolation of between 25 and 45 db over the frequency band was achieved; input impedance as seen from either port, 50 ohms, with VSWR less than 1.5.

This performance was certainly much superior to the performance of the first germanium isolator constructed and reported. Since the forward insertion loss of the Hall isolator was a function of the Hall angle in the sample, this angle was kept the same (about 20 degrees) in both isolators to provide a reasonably common basis for comparison. Although the isolation itself could not be very well predicted, the forward insertion loss was expected to improve, as the figures show. An improvement of 7 db was achieved under the same conditions by merely increasing the number of pairs of contacts per point in the new isolator.

The point thus had been established that multicontact Hall isolators were feasible in strip line and also that they performed with higher efficiency, as expected. Therefore, there should be no reason why the minimum insertion loss predicted as a function of the number of pairs of contacts per port could not be closely approached in practice. All

that is needed is a high  $\mu\beta$  (mobility  $\times$  magnetic induction) product to establish a Hall angle as close to 90 degrees as possible. For practical reasons  $\beta$  should be kept small. However, crystals with mobilities much superior than those of germanium can be used. Indium Arsenide is such a material, superior in over-all behavior to Indium Antimonide due to its high mobility combined with resistivity greater by a factor of 20 than that of the Indium Antimonide.

A Hall isolator made of multicontact samples of Indium Arsenide was recently designed and constructed. It employed an Indium Arsenide sample carrying eight pairs of contacts per port in a strip line arrangement designed for operation at the frequency of 600 mc.

So far only preliminary tests have been conducted on the isolator. Failure of the device to exhibit consistent nonreciprocity renders present data of dubious value. Several reasons were speculated on among which (1) the sample shape (rhombic, designed for a Hall angle of  $70^\circ$ ), (2) possible mobility reduction due to the many (thirty-two) ohmic contacts onto the InAs sample, (3) the very low resistance per port (about 15 ohms) of the sample. The first two reasons were disposed of promptly after a Ge sample, similar in every other respect to the InAs sample, was prepared and tested. The following results were obtained: over a bandwidth of about 160 mc/s, a forward insertion loss of 3.5 db approximately, but an isolation of only 3 db. VSWR was always less than 1.6 for 50 ohms input and output impedances. Although these results are far from being spectacular (the isolation is very low), they are, however, consistent and according to expectations, since the field available was only about 20 K Gauss while the field required theoretically for isolation (provided that the mobility of Ge is independent of the field strength) was computed to be about 90 K Gauss. Since isolation changes very rapidly in the neighborhood of the field value for which optimum isolation is obtained, the small isolation of the above device is reasonable. Moreover, should the field required be available, the forward insertion loss would be considerably lower.

Consistent with the above arguments were the results obtained from another eight-pairs-per-port Ge isolator, designed for  $50^\circ$  Hall angle, for which a theoretical isolating field of approximately 40 K Gauss was computed. With the 20 K Gauss field available, an insertion loss of about 5 db and an isolation of about 8.5 db were obtained over a frequency band of 140 mc/s, centered at 600 mc/s again. VSWR was better than 1.7 for 50 ohms input and output impedances. For this device the insertion loss is slightly inferior (expected of a sample designed for smaller Hall angle), but the isolation was much better than the  $70^\circ$  Hall isolator (also expected).



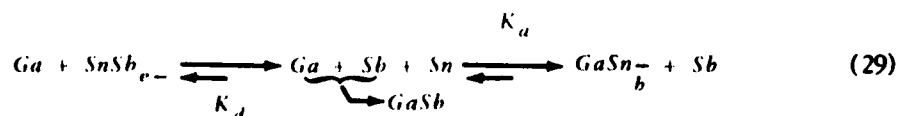
The above results suggest that the basic problem with the InAs isolator was the third of the reasons cited previously, that is, the very low resistance of the sample. In such a case, impedance transformations taking place through the quarter wavelength transformers directly attached by necessity to the contacts of the sample, usually reach some 7000:1 for which these lines behave essentially as short circuited resonant quarter wavelength lines. Because of the sharpness of resonance, slight deviations in resonance frequency between the input and output ports can be troublesome. One remedy would be to employ strip line boards of thickness smaller than 1/15 inch for smaller characteristic impedance lines, thereby reducing the transformation ratios above and broadening the resonance of the lines. However, the best remedy by far is to use higher resistivity materials as the germanium case has so successfully demonstrated. High mobilities to go along with high resistivities would constitute a perfect combination for materials to be used for practical Hall isolators to cover the whole spectrum, below the frequencies where ferrite isolators are not operable, down to d.c. Unfortunately the obtainable Indium Arsenide was of somewhat lower resistivity than had been anticipated, and thus adversely affected the experimental results. It is hoped that when purer InAs becomes available the predicted isolator performance will be fully realized.

### III. TUNNEL DIODES FOR MILLIMETER WAVE FREQUENCIES

#### A. FABRICATION AND TECHNOLOGY OF TUNNEL DIODES

Gallium antimonide tunnel diodes with peak to valley current ratios above 14 have been obtained at the lowest temperature yet (under 300°C) using novel tin 0.91 antimony 0.09 (weight fraction) alloy dots on zinc-doped ( $9.2 \times 10^{18}$  holes/cc) material. The low melting point of the alloy (246°C) makes it much easier to form contacts than state-of-the-art n-type alloys such as tin-tellurium.

The above observation may be the clearest example yet of the use of mass action influence to deliberately alter the amphoteric behavior of group IV elements to provide donors instead of acceptors (or vice versa) in III-V semiconductors. Since pure tin has been p-type in gallium antimonide, the following reactions go to the right for equal gallium and antimony concentrations.



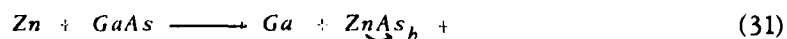
This means  $K/K_d = 1$  to give p-type material in the stoichiometric case. If, however, excess antimony is effectively present, the equilibrium may be tipped toward production of the SnSb donors. This becomes apparent from the defining equations:

$$\frac{[\text{SnSb}]}{K_d} \frac{[\text{Ga}]}{[\text{Ga}]} = \frac{[\text{Ga}][\text{Sb}][\text{Sn}]}{K_a} \frac{[\text{GaSn}]}{K_a} \frac{[\text{Sb}]}{[\text{Sb}]} \quad (30)$$

in which the brackets denote concentration in the melt. The  $K_a/K_d$  ratio might be expected to have an exponentially increasing behavior with temperature, to make it increasingly difficult to plant the tin on donor sites. Indeed the same alloy dots on tellurium-doped gallium antimonide ( $2.52 \times 10^{18}$  electrons/cc) have produced tunnel diodes of the opposite dopant orientation above 300°C. Under different conditions the very same alloy can produce an opposite doping effect.

The predominantly tin eutectics of zinc and cadmium which our last report mentions as novel p-type alloys for gallium antimonide have now been found also to give tunnel

diodes on n-type gallium arsenide. Since pure tin is predominantly n-type on gallium arsenide, ( $K_d/K_a > 1$ ) the success of these eutectics to produce acceptors may be another example of the appropriate tipping of equilibrium, this time in the other direction by an effective excess of gallium. Group II elements such as zinc or cadmium might be expected to yield gallium from gallium arsenide according to the reaction:



According to the previous relations excess gallium would help push the tin into acceptor sites thus explaining the observed behavior.

Tunnel diodes developed and supplied for circuit investigations included zinc-welded points to gallium arsenide as well as antimonide, and a low inductance sandwich structure with mica filled epoxy resin holding the diode pellet directly on the end of a brass stud.

Several experiments have shed more light on the behavior of group IV elements in GaSb. These are of interest because of the low compatibility of group VI donors with either the GaSb lattice, or with dot alloys. In an attempt to produce higher *donor* density, a GaSb single crystal was pulled from a melt with  $7 \times 10^{19} \text{ cm}^{-3}$  excess density of both tin and antimony. A hole density of  $1.48 \times 10^{17} \text{ cm}^{-3}$  was measured in a spectroscopic-analysis sample which showed from  $10^{17}$  to  $10^{18} \text{ cm}^{-3}$  atoms of tin. Because of segregation, the residue showed a much higher tin density, became polycrystalline, and indicated *n-type* by thermal probing.

In spite of the low equilibrium solubility and segregation coefficient of tin in GaSb, both pure tin and tin-antimony eutectic dots have given tunnel diodes on n-type GaSb ( $2.53 \times 10^{18} \text{ cm}^{-3}$  atoms of tellurium/cc). This indicates a high acceptor density and at least as high a tin density in the non-equilibrium recrystallized region under the dot. At lower temperatures, the tin-antimony but *not* the pure tin have given tunnel diodes on p-type GaSb ( $10^{17}$  to  $3 \times 10^{20} \text{ cm}^{-3}$  acceptors), thus indicating that antimony affects the amphoteric equilibrium as hypothesized in the last report. Measurements on such n on p units have shown less 1 pf/ma compared to the previous p on n units, which have from 1 to 10 pf/ma.

The low-doped base material just mentioned was only able to give tunnel diodes when a zinc-chloride-based flux was used. This indicates that significant zinc diffusion occurred during the few seconds alloying. Though initial peak-to-valley ratios up to 8 were

seen, these units are short-lived during mounting and after etching. Except for this, the higher impedance of such "surface diodes" would be a significant improvement.

Germanium-gold eutectic dots (m.p. 356°C) have given good-ratio tunnel diodes on n-type GaSb. Cross sections of etched units reveal that a plateau surrounds each dot as if a protective gold coat had diffused during alloying. The alloy's hardness makes it more difficult to contact than the tin-based dots.

## **B. MILLIMETER WAVE TUNNEL DIODE DETECTOR**

### **1. Introduction**

Considerable work has been done on tunnel-diode devices at UHF. Backward diodes have also been used as detectors and mixers at microwave frequencies.<sup>(8)</sup> The object of the project is to study the possibility of using tunnel diodes in various devices at millimeter and submillimeter wave frequencies.

This report covers the fabrication of the tunnel diodes and their use as small-signal detectors at mm wave frequencies. An analysis of small-signal detectors is also presented.

Present mm-wave crystal detectors have poor sensitivity, due at least in part to high series resistances. The tunnel diode was expected to be more sensitive as a detector because of the lower series resistance and larger nonlinear resistance, and greater sensitivity was actually obtained.

The diodes used in this project were formed in a tapered section of RG-98/U waveguide. The diodes were formed by passing a current pulse through the junction of the semiconductor and the metal contact. Figure 6 shows the arrangement of the diode in the waveguide and Figure 7 shows the circuit used in forming the diode. The voltage used in forming was approximately 100 volts. The resistance and capacitance used in the pulsing circuit varied according to the material with typical values of 100 to 500 ohms and 1 to 5 microfarads.

Most of the diodes used in this project were made of gallium-arsenide with a zinc wire because these materials gave reasonably good diodes and were easier to work with than the other materials tested. Units made from gallium arsenide have had peak-to-valley current ratios as large as 4 to 1. The peak currents can be controlled slightly by varying the capacitance and resistance used in the pulsing circuit. The units used in this experiment had peak currents of 2 ma to 30 ma.

(8) Eng, Sverre T., "Low-Noise Properties of Microwave Backward Diodes," I.R.E. Transactions on Microwave Theory and Techniques, September, 1961.

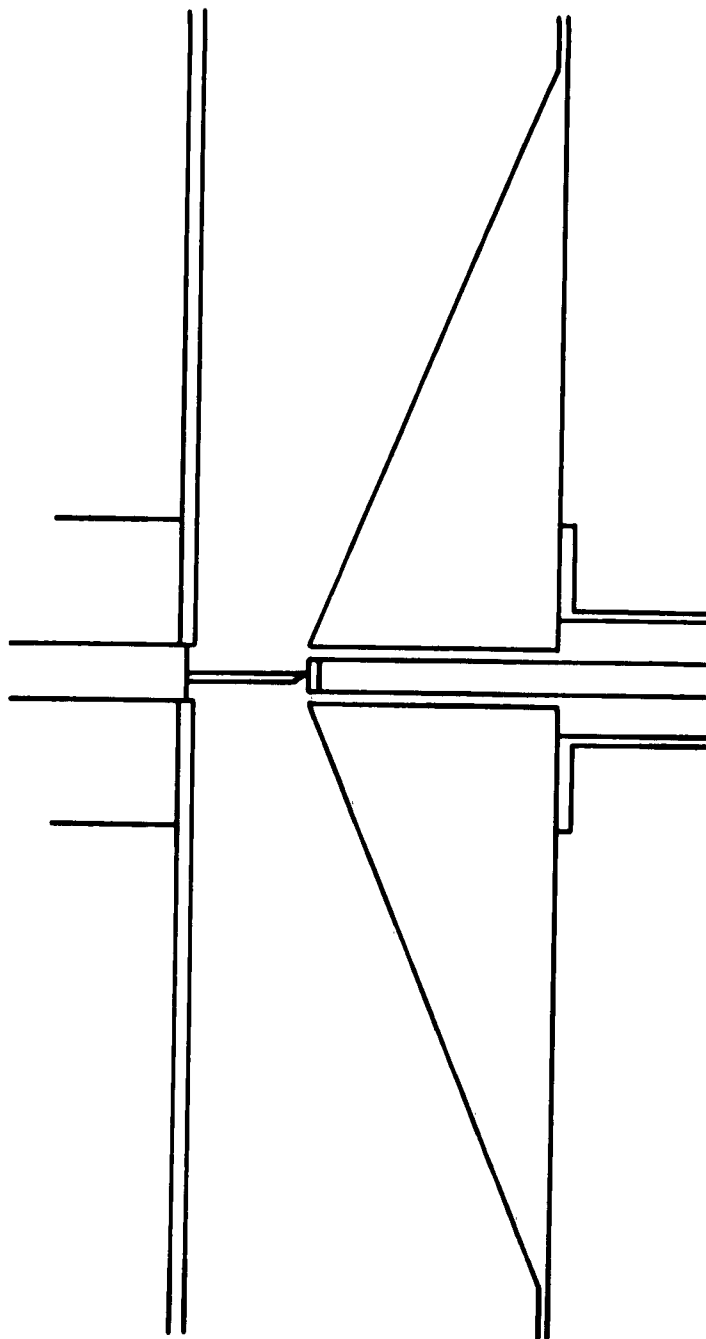


FIG. 6. DIODE ARRANGEMENT

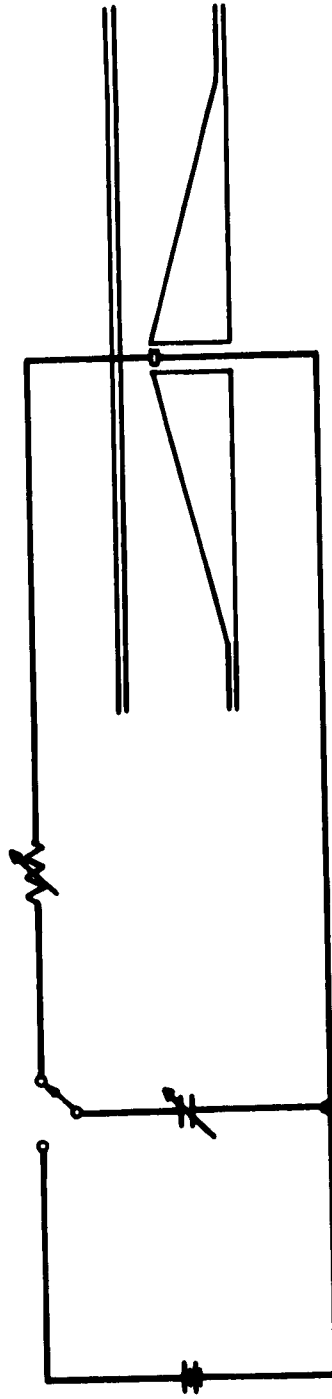


FIG. 7. DIODE FORMING CIRCUIT

Tunnel diodes were also made using germanium with an aluminum wire and gallium-antimonide with a zinc wire. The yield of good diodes was very small using these materials and the peak-to-valley current ratios were 2 to 1 or less. The peak currents for the gallium-antimonide units were from 10 ma to 25 ma and the peak currents for germanium were from 0.4 ma to 0.8 ma.

The impurity concentrations for gallium-arsenide and gallium-antimonide were about  $1$  to  $2 \times 10^{18}$  per cc with a resistivity of .001 to .0025 cm. The germanium crystals had a doping of about  $10^{18}$  per cc and resistivity of the order of .01 cm.

Tunnel diodes of all three semiconductor materials were operated at 55 Gc and all three showed an improvement in sensitivity over the 1N53 crystal detector used for comparison.

## 2. Analysis of Diode Detector

Figure 8a shows a possible detector circuit and Figure 8b is the accepted equivalent circuit for the tunnel diode. Assuming that the only connection of the output to the input  $a-a'$  is the phenomenon of rectification which occurs when r.f. power is absorbed at  $a-a'$ , expressions for the sensitivity can be obtained.

The r.f. power,  $P_i$ , absorbed by the diode is

$$P_i = \frac{|V_I|^2}{2} R_e \left\{ \frac{1}{Z} \right\} , \quad (33)$$

where

$$Z = r_s + j\omega L_s + \frac{1}{G + j\omega C} \quad (34)$$

and

$$G = \frac{1}{R} \quad (35)$$

The power into the diode can be written as

$$P_i = \frac{|V_I|^2}{2} \left[ \frac{G(1 + r_s G) + \omega^2 r_s C^2}{(1 + r_s G - \omega^2 L_s C)^2 + \omega^2 (L_s G + r_s C^2)} \right] \quad (36)$$

Expressing the junction voltage as a function of the input voltage gives

$$V_b = \frac{V_I}{(1 + r_s G - \omega^2 L_s C) + j\omega (L_s G + r_s C)} , \quad (37)$$

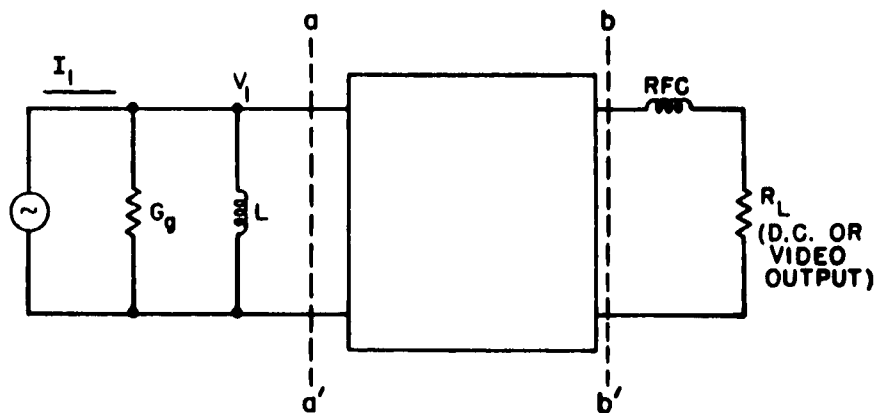


FIG. 8a- DETECTOR CIRCUIT

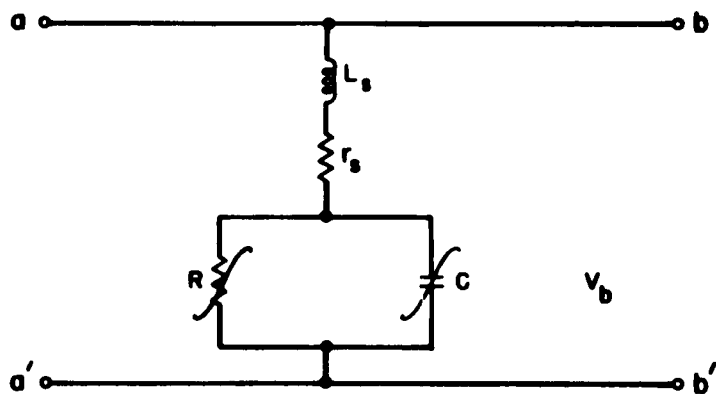


FIG. 8b- EQUIVALENT DIODE CIRCUIT



from which the input power can be expressed as

$$P_i = \frac{|V_b|^2}{2} G (1 + r_s G) + \omega^2 r_s C^2 \quad (38)$$

There are two sources of rectified short circuit current: the nonlinear resistance and the nonlinear capacitance. From the nonlinear capacitance the current is

$$i_{oc} = \frac{C V_b^2}{2 C_o r_s} \quad (39)$$

which is obtained from

$$q = C_o V + C V^2 \quad (40)$$

by averaging over a cycle. In this expression  $C_o$  is the capacitance at the bias point and  $C$  is the small signal nonlinear capacitance term. The nonlinear resistance gives

$$i_{oR} = \frac{V_b^2}{4} \frac{a}{R + r_s} \quad (41)$$

which is obtained from a Taylor series expansion and

$$a = \frac{f''(V_o)}{f'(V_o)} \quad (42)$$

where  $a$  is the small signal nonlinear resistance term. The total short circuit current is obtained by adding equations (39) and (41) to get

$$i_o = \frac{V_b^2}{4} \left( \frac{a}{R + r_s} + \frac{2C}{C_o r_s} \right) \quad (43)$$

The sensitivity,  $\beta$ , is defined as

$$\beta = \frac{i_o}{P_i} = \frac{1}{2} \frac{\frac{a}{R + r_s} + \frac{2C}{C_o r_s}}{G (1 + r_s G) + \omega^2 r_s C^2} \quad (44)$$

Replacing the short circuit with a load resistor allows the detection of an output voltage. The measureable voltage can be expressed as a function of the circuit parameters, also. From the nonlinear-capacitance term the voltage is

$$V_{oc} = \frac{C V_b^2}{2 C_o} \cdot \frac{R_o}{r_s + R_o}, \quad (45)$$

where  $R_o$  is the load resistance. The voltage obtained from the nonlinear resistance is

$$V_{oR} = \frac{a V_b^2}{4} \cdot \frac{R_o}{R_o + R + r_s}. \quad (46)$$

The total output voltage is then

$$V_{oT} = \frac{V_b^2 R_o}{4(R_o + r_s)} \left( \frac{a}{1 + \frac{R}{R_o + r_s}} + \frac{2C}{C_o} \right) \quad (47)$$

Rewriting the output voltage in terms of the input voltage gives

$$V_{oT} = \frac{V_i^2 R_o}{1 + (R_o + r_s)} \cdot \frac{a}{1 + \frac{R}{R_o + r_s}} + \frac{2C}{C_o} \cdot \frac{1}{\left(1 - \omega^2 \frac{L_s C}{1 + r_s G}\right)^2 + \omega^2 \left(\frac{L_s G + r_s C}{1 + r_s G}\right)^2} \quad (48)$$

Normalizing the output voltage with respect to the input power gives

$$V'_{oT} = \frac{K_o}{K_1^2 \omega^4 + (K_2 - 2K_1) \omega^2 + 1}, \quad (49)$$

where

$$K_o = \left( \frac{R_o}{R_o + r_s} \right) \left( \frac{a}{1 + \frac{R}{R_o + r_s}} + \frac{2C}{C_o} \right) \left( \frac{1}{1 + r_s G} \right)^2 \quad (50)$$

$$K_1 = \frac{L_s C}{1 + r_s G}, \text{ and} \quad (51)$$

$$K_2 = \left( \frac{L_s G + r_s C}{1 + r_s G} \right)^2 \quad (52)$$

### 3. Theoretical Results

Figure 9 gives the behavior of equation 49 for the various circuit parameters that might be expected from various kinds of diodes. The three curves are arrived at by using the following parameters which can be expected from tunnel diodes biased near the peak current point (A), backward diodes (B), and ordinary crystals (C):

A—

$$\begin{aligned} R_o &= 50 \\ R &= 50 \\ L_s &= 10^{-9} \text{ h} \\ C &= .5 \times 10^{-12} \text{ f} \\ a &= 200^{(9)} \\ C/C_o &= 1^{(10)} \end{aligned}$$

B—

$$\begin{aligned} R_o &= 50 \\ R &= 100 \\ r_s &= 5 \\ L_s &= 10^{-9} \text{ h} \\ C &= 10^{-12} \text{ f} \\ a &= 50^{(8)} \\ C/C_o &= 1 \end{aligned}$$

(9) H. J. Prager and K. K. N. Chang, "The Effect of Large Pump Voltage on Tunnel Diode Down Converter Performance," RCA Review, September, 1961.

(10) K. K. N. Chang and S. Bloom, "A Parametric Amplifier Using Lower-Frequency Pumping," Proceedings of the I.R.E., July, 1958.

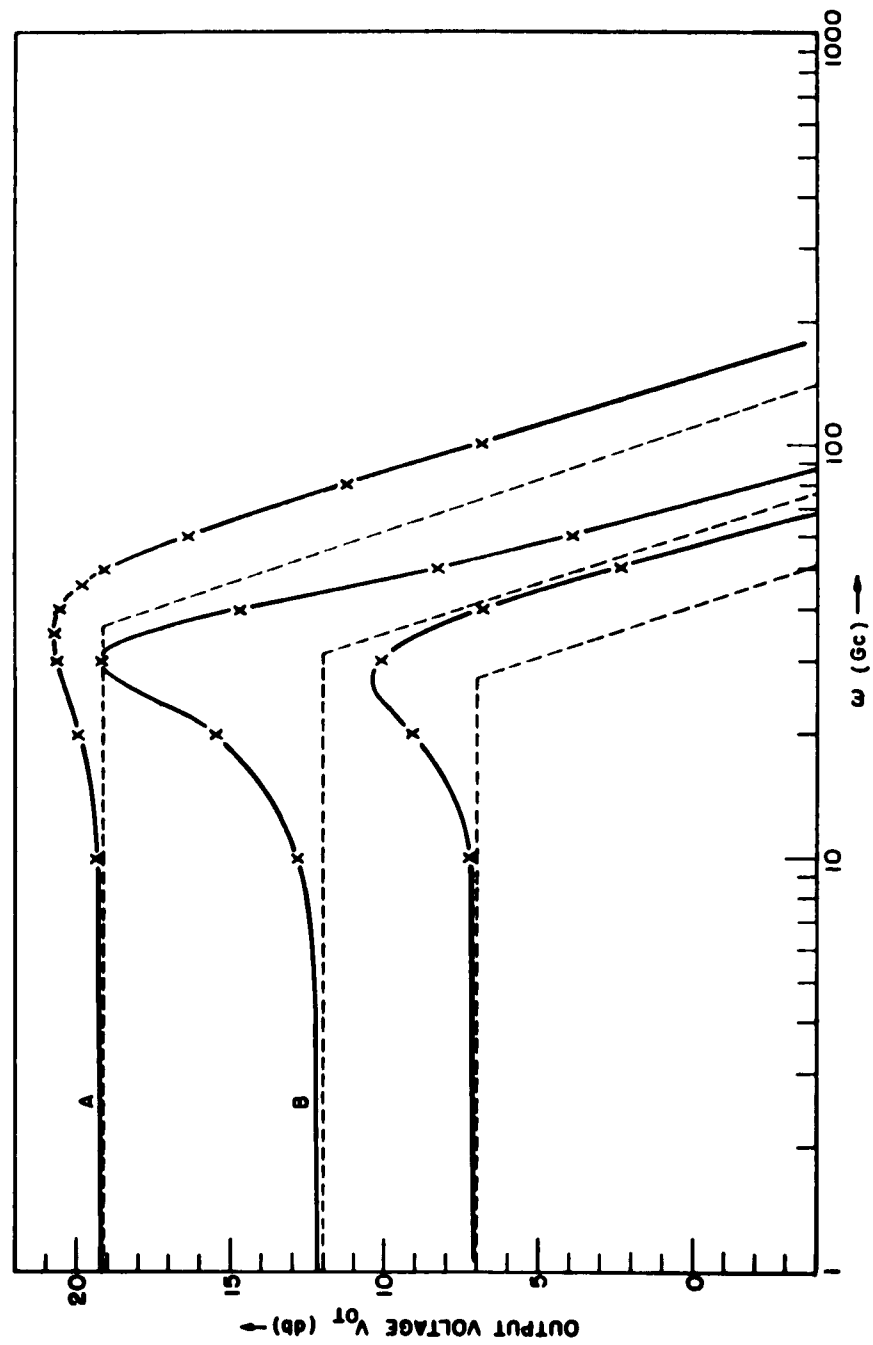


**FIG. 9. OUTPUT FROM VARIOUS DETECTOR DIODES**

$$\begin{aligned}
 C- \quad R_o &= 50 \\
 R &= 200 \\
 r_s &= 20 \\
 L_s &= 10^{-9} \\
 C &= 10^{-12} \\
 a &= 25^{(11)} \\
 C/C_o &= 1
 \end{aligned}$$

Equation 48 indicates how the various parameters affect the operation of a detector diode. In the case of a forward-biased diode the term accounting for the nonlinear capacitance can be neglected since it contributes less than two per cent of the total output.

The nonlinear resistance coefficient used in this calculation was taken from the actual curve of a diode used. With improvement of the diodes it seems quite likely that the value of this coefficient could be increased to the order of 400.

#### 4. Experimental Results

The tunnel diode detector has shown considerable improvement in sensitivity over commercially available detectors at 55 Gc, where sensitivity is defined as the power required to make the output signal just equal to the noise level of the detector.

The tunnel diode detectors were compared to a 1N53 crystal. All three materials used had better sensitivity than the 1N53 but gallium-arsenide and gallium-antimonide showed greater improvement than germanium. Typical figures for the materials used were: germanium - 8 to 15 db improvement, gallium-antimonide - 15 to 25 db improvement, and gallium-arsenide - 15 to 22 db improvement. As can be seen, the gallium-antimonide gave the best results but the gallium-arsenide diodes were more consistent and considerably easier to make, so most of the work was done on gallium-arsenide.

Biasing the tunnel diode in the forward direction improved the sensitivity. An improvement in sensitivity of as much as 5 db could be obtained by biasing the diode near the peak current point as compared to the sensitivity at zero bias. The improvement is to be expected since this is where the greatest nonlinearity is exhibited.

The noise performance of tunnel diodes is also better than that of an ordinary crystal. This is expected because the noise performance is related directly to the figure

(11) H. C. Torrey and C. A. Whitmer, "Crystal Rectifiers," McGraw-Hill Book Co., Inc. New York, N.Y., 1948.

of merit of a diode which is itself related to the current sensitivity. As seen before, the current sensitivity of a tunnel diode is considerably better than that of an ordinary diode.

Figure 10 shows some of the apparatus used in this project. The operation of the experimental diode and of the 1N53 crystal was studied at the same point in the circuit. The bolometer allowed the monitoring of the power levels.

The results obtained so far indicate that the tunnel diode can be used quite effectively at mm wave frequencies.

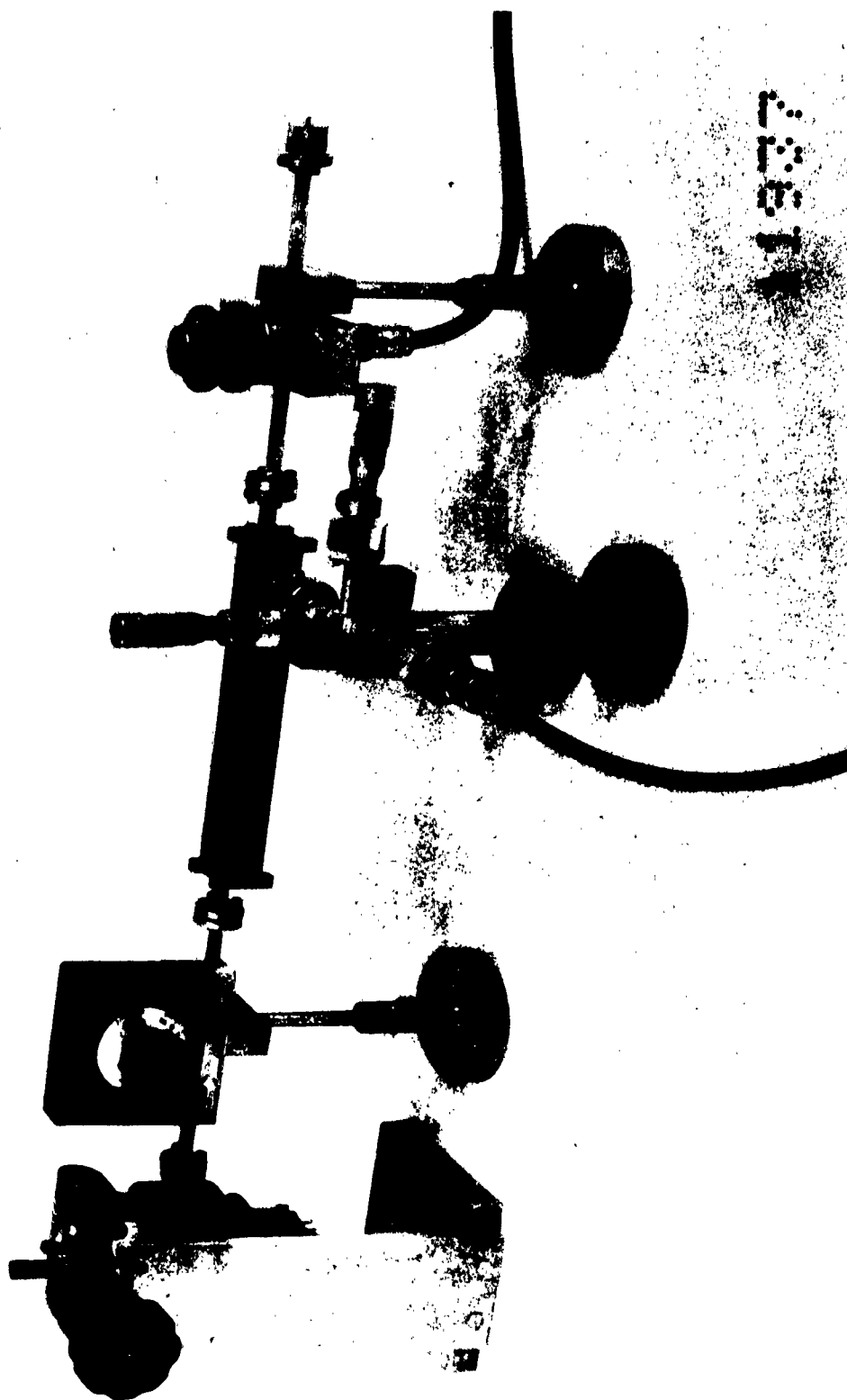


FIG. 10.

<p>Electronic Research Directorate, Air Force Cambridge Research Laboratories. AFCRL-62-918. THEORETICAL AND EXPERIMENTAL STUDY OF THE COMBINED HALL-MAGNETO RESISTANCE EFFECT. Scientific Report No. 2, 31 Oct. 62, 42p. incl. illus. 11 ref. Unclassified Report</p> <p>A new group of microwave devices based on the Hall-Effect is being sought. A frequency converter at the S-Band region was built and gave a conversion loss of 20 to 30 db. A novel scheme based entirely on enhanced interaction between the Hall sample and its associated circuitry was analytically examined. The first experimental embodiment of this scheme seems to have yielded a small net gain at a frequency of 3730 mc. The report also includes the fabrication techniques for millimeter wave tunnel diodes (as detectors). An improvement in sensitivity of 25 db as compared to ordinary crystal detectors has been obtained.</p>	<ol style="list-style-type: none"> <li>1. Solid State Microwave Amplifiers.</li> <li>2. Solid State Microwave Converters</li> <li>3. Tunnel Diode Detector</li> </ol> <ol style="list-style-type: none"> <li>I. Contract AF19(628)262</li> <li>II. Radio Corporation of America, Princeton, N.J.</li> <li>III. K.K.N. Chang, P. E. Chase and H.J. Prager</li> </ol>
<p>Electronic Research Directorate, Air Force Cambridge Research Laboratories. AFCRL-62-918. THEORETICAL AND EXPERIMENTAL STUDY OF THE COMBINED HALL-MAGNETO RESISTANCE EFFECT. Scientific Report No. 2, 31 Oct. 62, 42p. incl. illus. 11 ref. Unclassified Report</p> <p>A new group of microwave devices based on the Hall-Effect is being sought. A frequency converter at the S-Band region was built and gave a conversion loss of 20 to 30 db. A novel scheme based entirely on enhanced interaction between the Hall sample and its associated circuitry was analytically examined. The first experimental embodiment of this scheme seems to have yielded a small net gain at a frequency of 3730 mc. The report also includes the fabrication techniques for millimeter wave tunnel diodes (as detectors). An improvement in sensitivity of 25 db as compared to ordinary crystal detectors has been obtained.</p>	<ol style="list-style-type: none"> <li>1. Solid State Microwave Amplifiers.</li> <li>2. Solid State Microwave Converters</li> <li>3. Tunnel Diode Detector</li> </ol> <ol style="list-style-type: none"> <li>I. Contract AF19(628)262</li> <li>II. Radio Corporation of America, Princeton, N.J.</li> <li>III. K.K.N. Chang, P. E. Chase and H.J. Prager</li> </ol>
<p>Electronic Research Directorate, Air Force Cambridge Research Laboratories. AFCRL-62-918. THEORETICAL AND EXPERIMENTAL STUDY OF THE COMBINED HALL-MAGNETO RESISTANCE EFFECT. Scientific Report No. 2, 31 Oct. 62, 42p. incl. illus. 11 ref. Unclassified Report</p> <p>A new group of microwave devices based on the Hall-Effect is being sought. A frequency converter at the S-Band region was built and gave a conversion loss of 20 to 30 db. A novel scheme based entirely on enhanced interaction between the Hall sample and its associated circuitry was analytically examined. The first experimental embodiment of this scheme seems to have yielded a small net gain at a frequency of 3730 mc. The report also includes the fabrication techniques for millimeter wave tunnel diodes (as detectors). An improvement in sensitivity of 25 db as compared to ordinary crystal detectors has been obtained.</p>	<ol style="list-style-type: none"> <li>1. Solid State Microwave Amplifiers</li> <li>2. Solid State Microwave Converters</li> <li>3. Tunnel Diode Detector</li> </ol> <ol style="list-style-type: none"> <li>I. Contract AF19(628)262</li> <li>II. Radio Corporation of America, Princeton, N.J.</li> <li>III. K.K.N. Chang, P. E. Chase and H.J. Prager</li> </ol>
<p>Electronic Research Directorate, Air Force Cambridge Research Laboratories. AFCRL-62-918. THEORETICAL AND EXPERIMENTAL STUDY OF THE COMBINED HALL-MAGNETO RESISTANCE EFFECT. Scientific Report No. 2, 31 Oct. 62, 42p. incl. illus. 11 ref. Unclassified Report</p> <p>A new group of microwave devices based on the Hall-Effect is being sought. A frequency converter at the S-Band region was built and gave a conversion loss of 20 to 30 db. A novel scheme based entirely on enhanced interaction between the Hall sample and its associated circuitry was analytically examined. The first experimental embodiment of this scheme seems to have yielded a small net gain at a frequency of 3730 mc. The report also includes the fabrication techniques for millimeter wave tunnel diodes (as detectors). An improvement in sensitivity of 25 db as compared to ordinary crystal detectors has been obtained.</p>	<ol style="list-style-type: none"> <li>1. Solid State Microwave Amplifiers</li> <li>2. Solid State Microwave Converters</li> <li>3. Tunnel Diode Detector</li> </ol> <ol style="list-style-type: none"> <li>I. Contract AF19(628)262</li> <li>II. Radio Corporation of America, Princeton, N.J.</li> <li>III. K.K.N. Chang, P. E. Chase and H.J. Prager</li> </ol>



<p>Electronic Research Directorate, Air Force Cambridge Research Laboratories. AFCRL-62-918. THEORETICAL AND EXPERIMENTAL STUDY OF THE COMBINED HALL-MAGNETO RESISTANCE EFFECT. Scientific Report No. 2, 31 Oct. 62, 42p. incl. illus. 11 ref. Unclassified Report</p> <p>A new group of microwave devices based on the Hall-Effect is being sought. A frequency converter at the S-Band region was built and gave a conversion loss of 20 to 30 db. A novel scheme based entirely on enhanced interaction between the Hall sample and its associated circuitry was analytically examined. The first experimental embodiment of this scheme seems to have yielded a small net gain at a frequency of 3730 mc. The report also includes the fabrication techniques for millimeter wave tunnel diodes (as detectors). An improvement in sensitivity of 25 db as compared to ordinary crystal detectors has been obtained.</p>	<p>1. Solid State Microwave Amplifiers. 2. Solid State Microwave Converters 3. Tunnel Diode Detector</p> <p>I. Contract AF19(628)262 II. Radio Corporation of America, Princeton, N.J. III. K.K.N. Chang, P. E. Chase and H.J. Prager</p>	<p>Electronic Research Directorate, Air Force Cambridge Research Laboratories. AFCRL-62-918. THEORETICAL AND EXPERIMENTAL STUDY OF THE COMBINED HALL-MAGNETO RESISTANCE EFFECT. Scientific Report No. 2, 31 Oct. 62, 42p. incl. illus. 11 ref. Unclassified Report</p> <p>A new group of microwave devices based on the Hall-Effect is being sought. A frequency converter at the S-Band region was built and gave a conversion loss of 20 to 30 db. A novel scheme based entirely on enhanced interaction between the Hall sample and its associated circuitry was analytically examined. The first experimental embodiment of this scheme seems to have yielded a small net gain at a frequency of 3730 mc. The report also includes the fabrication techniques for millimeter wave tunnel diodes (as detectors). An improvement in sensitivity of 25 db as compared to ordinary crystal detectors has been obtained.</p>	<p>1. Solid State Microwave Amplifiers 2. Solid State Microwave Converters 3. Tunnel Diode Detector</p> <p>I. Contract AF19(628)262 II. Radio Corporation of America, Princeton, N.J. III. K.K.N. Chang, P. E. Chase and H.J. Prager</p>
<p>Electronic Research Directorate, Air Force Cambridge Research Laboratories. AFCRL-62-918. THEORETICAL AND EXPERIMENTAL STUDY OF THE COMBINED HALL-MAGNETO RESISTANCE EFFECT. Scientific Report No. 2, 31 Oct. 62, 42p. incl. illus. 11 ref. Unclassified Report</p> <p>A new group of microwave devices based on the Hall-Effect is being sought. A frequency converter at the S-Band region was built and gave a conversion loss of 20 to 30 db. A novel scheme based entirely on enhanced interaction between the Hall sample and its associated circuitry was analytically examined. The first experimental embodiment of this scheme seems to have yielded a small net gain at a frequency of 3730 mc. The report also includes the fabrication techniques for millimeter wave tunnel diodes (as detectors). An improvement in sensitivity of 25 db as compared to ordinary crystal detectors has been obtained.</p>	<p>1. Solid State Microwave Amplifiers. 2. Solid State Microwave Converters 3. Tunnel Diode Detector</p> <p>I. Contract AF19(628)262 II. Radio Corporation of America, Princeton, N.J. III. K.K.N. Chang, P. E. Chase and H.J. Prager</p>	<p>Electronic Research Directorate, Air Force Cambridge Research Laboratories. AFCRL-62-918. THEORETICAL AND EXPERIMENTAL STUDY OF THE COMBINED HALL-MAGNETO RESISTANCE EFFECT. Scientific Report No. 2, 31 Oct. 62, 42p. incl. illus. 11 ref. Unclassified Report</p> <p>A new group of microwave devices based on the Hall-Effect is being sought. A frequency converter at the S-Band region was built and gave a conversion loss of 20 to 30 db. A novel scheme based entirely on enhanced interaction between the Hall sample and its associated circuitry was analytically examined. The first experimental embodiment of this scheme seems to have yielded a small net gain at a frequency of 3730 mc. The report also includes the fabrication techniques for millimeter wave tunnel diodes (as detectors). An improvement in sensitivity of 25 db as compared to ordinary crystal detectors has been obtained.</p>	<p>1. Solid State Microwave Amplifiers 2. Solid State Microwave Converters 3. Tunnel Diode Detector</p> <p>I. Contract AF19(628)262 II. Radio Corporation of America, Princeton, N.J. III. K.K.N. Chang, P. E. Chase and H.J. Prager</p>